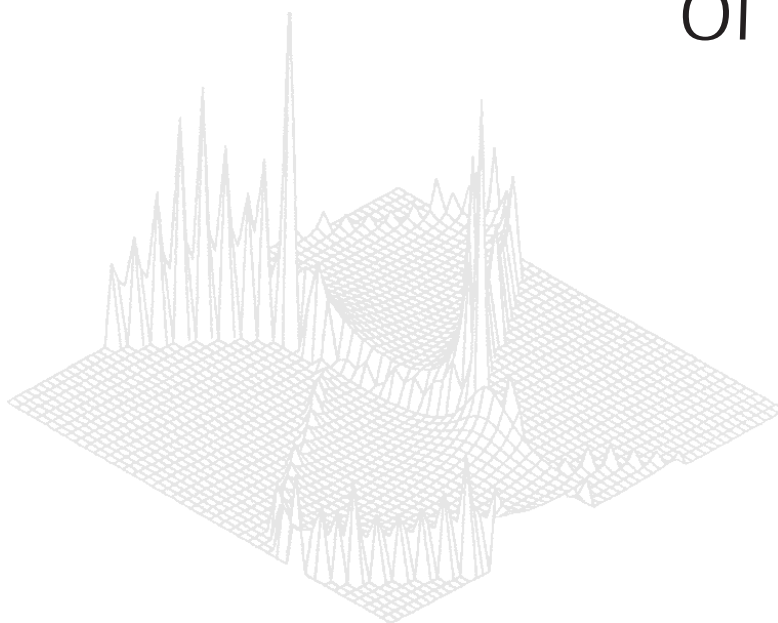

CSIRO PUBLISHING

Australian Journal of Physics

Volume 53, 2000
© CSIRO 2000



A journal for the publication of
original research in all branches of physics

www.publish.csiro.au/journals/ajp

All enquiries and manuscripts should be directed to

Australian Journal of Physics

CSIRO PUBLISHING

PO Box 1139 (150 Oxford St)

Collingwood

Vic. 3066

Australia

Telephone: 61 3 9662 7626

Facsimile: 61 3 9662 7611

Email: peter.robertson@publish.csiro.au



Published by **CSIRO PUBLISHING**
for CSIRO and
the Australian Academy of Science



Real Critical Current Density and Material Power Law of $\text{YBa}_2\text{Cu}_3\text{O}_{7-\delta}$ Epitaxial Thin Film

Lei Shan, Sahr Augustine Aruna,^A Xiao-Nong Xu, Zhi-He Wang and Xin Jin

Department of Physics and National Laboratory of Solid State Microstructure, Nanjing University, Nanjing 210 008, China.

^ADepartment of Physics, Fourah Bay College, University of Sierra Leone, Freetown, Sierra Leone.

Abstract

The current–voltage characteristics have been measured on a $\text{YBa}_2\text{Cu}_3\text{O}_{7-\delta}$ epitaxial thin film. Using a material power law, we determine the temperature and field dependencies of the characteristic pinning potential U_J and the real critical current density J_c at different fields and temperatures. It is shown that J_c is completely different from the conventional critical current density J_E , which is determined by the electronic-field criterion. Thus, the time-honoured electronic-field criterion is no longer reasonable for high- T_c superconductors. By further investigation of the results of J_c and U_J , we are able to present a physical picture of the transformation of the pinning potential well with increasing temperature and hence determine the transition point from vortex-glass phase to vortex-liquid phase.

1. Introduction

Due to the high critical temperature, the strong anisotropy and the short coherence length, a rich vortex-matter phase diagram exists in the mixed state of high- T_c superconductors (HTSC). The complicated dynamic behaviours of the vortex phases in HTSC arise from competition between the driven force and various energies such as the thermal energy, vortex interaction energy, pinning energy and coupling energy between layers (Crabtree and Nelson 1997). An important early step in dynamical vortex studies is the characterisation of the various steady-motion states in the dynamic phase diagram (Koshelev and Vinokur 1994; Giamarchi and Le Doussal 1996), which is closely associated with the critical current of HTSC.

The conventional critical current density J_E is determined as follows: (a) It can be derived from the width of the magnetic hysteresis loops using the basic assumption of the Bean critical state model. (b) It can be determined from the current–voltage characteristics (CVC) by selecting an electronic-field criterion (EFC). However, these two methods assume that the electric field arises abruptly at the critical current density, which is adequate only for low- T_c superconductors. For HTSC, due to giant flux creep, the electronic-field changes more slowly with decreasing current density than in low- T_c superconductors. Therefore, the conventional critical current density J_E should not be regarded as the real critical current density J_c in theoretical analyses for HTSC. Because J_c is a necessary parameter for flux pinning theory to scale the effective pinning potential and is the threshold to separate a rest phase (flux creep regime) from a moving phase (flux flow regime) in the dynamic phase diagram, then the determination of J_c is of principal importance in research on vortex matter in HTSC. Recently, new methods have been proposed to extract J_c , such as the generalised inversion scheme (GIS) (Wen and Zhao 1995) and the Bardeen–Stephen

criterion (Bondarenko *et al.* 1998). But to our knowledge, because there is no theoretical discussion about J_c and J_E and a quantitative comparison between them, the EFC is still widely used in investigations on the vortex matter in HTSC. The inadequate substitution of J_E for J_c and the arbitrary choice of EFC from 10^{-1} to 10^{-5} V m $^{-1}$ has inevitably brought some dubious conclusions (Mannhart *et al.* 1988; Mankiewich *et al.* 1989; Sueyoshi *et al.* 1998; Doyle *et al.* 1998) and covered up the physical implication of J_c .

In this paper, the $E \sim J$ relations of YBa $_2$ Cu $_3$ O $_{7-\delta}$ epitaxial film are presented for various magnetic fields and temperatures around the transition from the vortex-glass phase to vortex-liquid phase (for simplicity, hereafter referred to as the GL transition). In order to avoid the 2D vortex regime and the demagnetisation effect, we have applied a magnetic field parallel to the ab plane of the sample. Using a theoretical material power law (MPL) (Brandt 1996, 1997; Yazawa *et al.* 1998), we obtain the temperature and magnetic field dependent characteristic pinning potential $U_J(T, H)$ and real critical current density $J_c(T, H)$. By comparing J_c with J_E , we show the irrationality of the EFC. Furthermore, based on the $U_J \sim J_c$ relation, we interpret the temperature induced GL transition from the viewpoint of the pinning potential well of the vortex line.

2. Experimental

The highly c -axis oriented YBa $_2$ Cu $_3$ O $_{7-\delta}$ epitaxial thin film in this work was prepared on a SrTiO $_3$ substrate by DC magnetron sputtering (Jakob 1991). The X-ray diffraction pattern reveals that the film is highly c -axis oriented and epitaxial. By using the standard four probe method, we have measured DC CVC on a YBCO film which is 200 nm thick, with an etched 200 μ m \times 60 μ m bridge. The direct current is supplied by a Keithley 220 current source and the voltage is measured by a Keithley 182 nanovoltmeter. The temperature was stabilised at better than ± 0.01 K during the measurements.

The isothermal $E \sim J$ curves of the YBa $_2$ Cu $_3$ O $_{7-\delta}$ epitaxial thin film were measured for the configuration of $H \parallel ab$ plane and $H \perp J$, where J is the in-plane current density. Fig. 1a shows the $\ln E \sim \ln J$ curves for various temperatures from 82.56 to 86.98 K at the fixed magnetic field of 8 T, and Fig. 1b shows the $\ln E \sim \ln J$ curves for various fields from 1 to 6 T at the fixed temperature of 87.82 K. It is clear that, in this temperature or field region, $\ln E$ depends linearly on $\ln J$, which is consistent with the MPL elaborated below.

3. Determination of Characteristic Pinning Potential and Critical Current Density

In order to reveal the characteristics of flux creep in HTSC under the driven force caused by applied current, the key problem is to determine the effective pinning potential. This has attracted a lot of theoretical and experimental effort. The general form has been proposed by Malozemoff (1991), Griessen *et al.* (1997) and Schnack *et al.* (1993):

$$U_{eff}(T, H, J) = \frac{U_J(T, H)}{\mu(T, H)} \left[\left(\frac{J_c(T, H)}{J} \right)^{\mu(T, H)} - 1 \right], \quad (1)$$

where $U_J(T, H)$ is the characteristic pinning potential, $J_c(T, H)$ is the real critical current density corresponding to zero activation energy, and μ is an exponent which has various values corresponding to different models. As one of the special cases, the following logarithmic model suggested by Zeldov *et al.* (1990) can be derived when μ tends to zero:

$$U_{eff}(T, H, J) = U_J(T, H) \ln \left(\frac{J_c(T, H)}{J} \right). \quad (2)$$

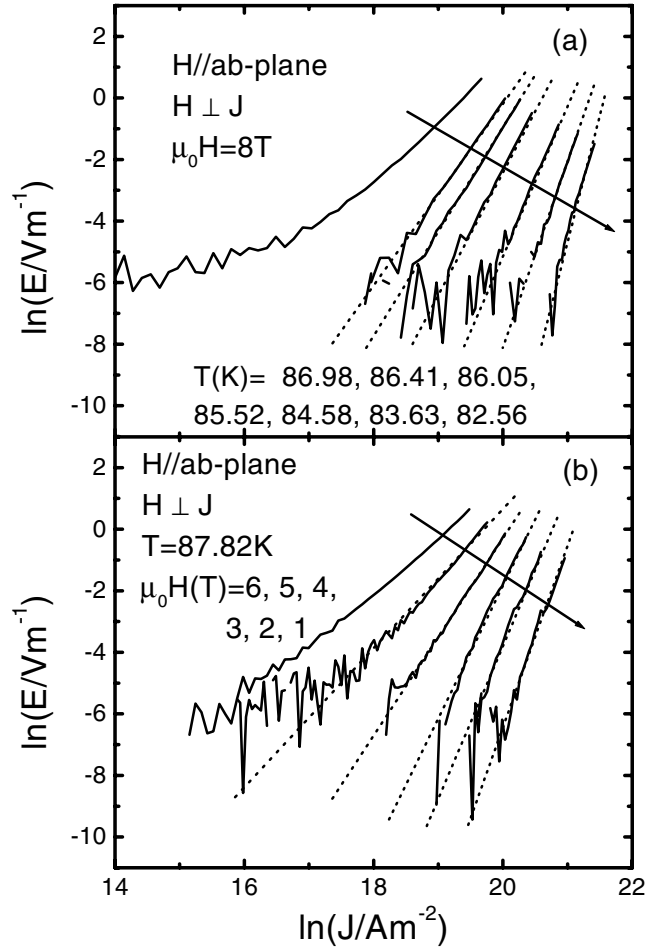


Fig. 1. (a) Current–voltage characteristics measured at $\mu_0 H = 8 T$ for various temperatures (82.56–86.98 K). (b) CVC measured at $T = 87.82 K$ for various magnetic fields (1–6 T). The dotted lines indicate the linear fit for the $\ln E \sim \ln J$ curves.

According to the Anderson (1966) phase-slip theory and the Arrhenius law, the energy loss equation of the super current can be written as

$$E = v_0 L B \exp \left[- \frac{U_{eff}(T, H, J)}{kT} \right], \quad (3)$$

where v_0 is the attempt frequency of vortex line hopping, L is the average distance of hopping, k is the Boltzmann constant, and E is the electronic field caused by vortex motion with velocity $V = v_0 L \exp[-U_{eff}(T, H, J)/kT]$. Applying equation (2) in (3) we have

$$E = v_0 L B \left[\frac{J}{J_c(T, H)} \right]^{U_j(T, H)/kT}. \quad (4)$$

Because the parameters v_0L and U_J in this power law are closely associated with the material properties, we call equation (4) the material power law (MPL), which is similar to the following experimental power law (Yazawa *et al.* 1998):

$$E = E_c \left(\frac{J}{J_E} \right)^n, \quad (5)$$

where J_E is the conventional critical current density depending on the choice of the electronic-field criterion E_c . This power law is observed in numerous experiments and was used in theories on creep (Vinokur *et al.* 1991; Gurevich and Brandt 1994; Schuster *et al.* 1995a), flux penetration (Schuster *et al.* 1994a, 1994b, 1995b, 1996) and AC susceptibility (Rhyner 1993; Gilchrist and van der Beek 1994; Brandt 1995; Schuster *et al.* 1995, 1996). The value of E_c in recent reports ranges from 10^{-5} to 10^{-4} V m⁻¹ (Wen and Zhao 1995; Higgins and Bhattacharya 1996; Doyle *et al.* 1998). However, it should be noted that the time-honoured EFC is unreasonable to determine the critical current density for HTSC, because the decay of voltage with decreasing current is not so abrupt as in conventional superconductors. In order to obtain the real critical current density of HTSC, we must adopt equation (4) instead of (5). Considering our previous discussions on YBa₂Cu₃O_{7-δ} (Shan *et al.* 1999), we have $v_0L = 6.1$ m s⁻¹ and hence obtain $J_c^E/J_c^r = (E_c/6.1B)^{1/n}$ by combining (4) and (5). Now, we rewrite the MPL as

$$\ln E = \frac{U_J}{kT} \ln J + \ln v_0LB - \frac{U_J}{kT} \ln J_c. \quad (6)$$

It is obvious that $U_J(T, H)$ can be calculated from the slope of $\ln E \sim \ln J$ curves and then J_c can be determined simultaneously from the intercepts. Here we should point out that the MPL is valid only for the linear relation of $\ln E \sim \ln J$. It is known that the GL transition is reflected by the transition of the $\ln E \sim \ln J$ characteristic from negative curvature to positive curvature (Brown 2000). However, because of the limited measuring precision, the $\ln E \sim \ln J$ curves exhibit linear behaviour around this transition. Therefore, from Fig. 1, we could declare that our experiment has included the GL transition because of the small curvature transition, and hence the following discussion is focussed on the GL transition.

4. Results and Discussion

The temperature and field dependencies of U_J are represented in Fig. 2 by the solid squares and open circles respectively. It is noted that both $U_J(H)$ and $U_J(T)$ obey the linear decay law around the GL transition. Figs 3a and 3b show the temperature and field dependencies of J_c , J_E^1 (with $E_c = 10^{-2}$ V m⁻¹), and J_E^2 (with $E_c = 10^{-4}$ V m⁻¹). We find that the conventional critical current density J_E is almost 1 ~ 2 orders smaller than the real critical current density J_c , and the deviation of J_E from J_c becomes more and more severe with increasing temperature or field. Moreover, the arbitrary choice of the EFC (E_c) will bring about the uncertainty of J_E and hence leads to the loss of true information about the pinning characteristics of HTSC.

In the following we reveal the physical implications of the U_J and J_c we have obtained. It is noted that the GL transition point is difficult to determine from the typical CVC as shown in Fig. 1 and the continued $U_J(T, H)$ in Fig. 2 or $J_c(T, H)$ in Fig. 3. However, by

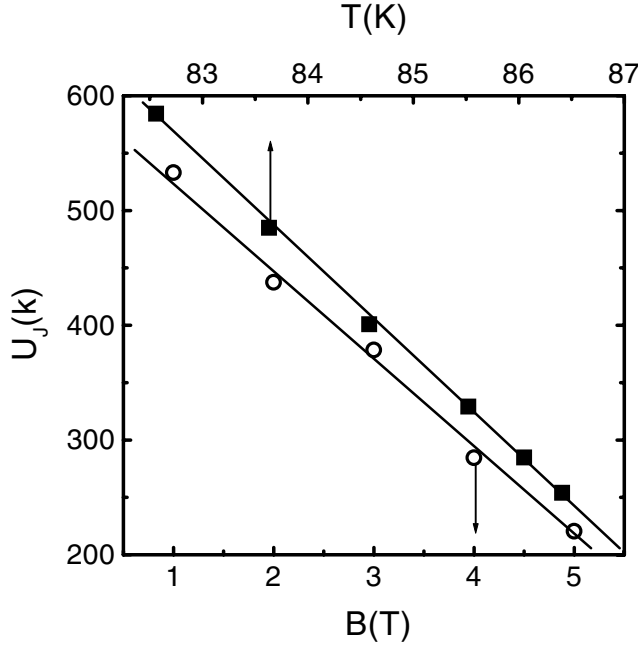


Fig. 2. Temperature and field dependencies of the characteristic pinning potential U_J .

investigating the relation between U_J and J_c , we were able to find the GL transition point on the viewpoint of the variational shape of the pinning potential well.

We note that the shape of the pinning potential well corresponding to the MPL should be described as follows (Zeldov *et al.* 1990):

$$U_0(x) = \begin{cases} \alpha x/x_0, & 0 \leq x \leq x_0 \\ \alpha[\ln(x/x_0) + 1], & x > x_0 \end{cases} \quad (7)$$

where x is the spatial coordinate and α and x_0 are the energy and position scaling factors respectively. In this case, the vortex line potential is localised in a narrow cone-like structure which exhibits a broad logarithmic decay and α represents the characteristic pinning potential U_J , which is equal to $U_0(x_0)$, as shown in Fig. 4b. Now we consider the general definition of the effective pinning potential:

$$U_{eff} = \max[U_0(x) - V_c B J x] \quad (8)$$

in which V_c is the correlation volume. Equation (8) indicates that the shape of the pinning potential well is a crucial factor in determining the value of J_c , for the critical depinning force is derived from the zero effective pinning potential.

Applying equation (7) to (8), we have $J_c = U_J/x_0$, that is, if x_0 is constant, U_J should decay linearly with decreasing J_c . The $U_J \sim J_c$ relation is presented in Fig. 4a, where the fixed magnetic field of 8 T insures that the value of a (where a is the separation between the adjacent wells, i.e. $a \propto \sqrt{1/B}$) is invariable. It is noted that U_J depends on J_c linearly above the transition temperature T_{tr} , while below T_{tr} the dependence of U_J on J_c becomes weaker. This contradicts the above prediction by assuming a fixed x_0 , so we must take into account the change of x_0 with temperature. The physical mechanism that may result in

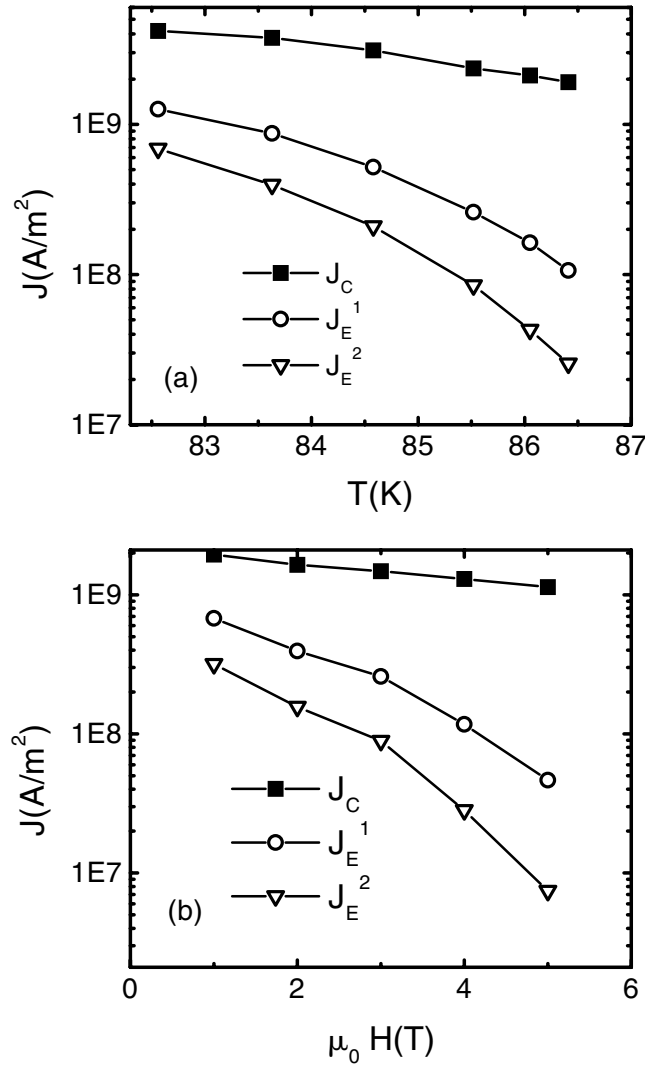


Fig. 3. (a) Temperature dependence of J_c , J_E^1 ($E_c = 10^{-2} \text{ V m}^{-1}$) and J_E^2 ($E_c = 10^{-4} \text{ V m}^{-1}$). (b) Field dependence of J_c , J_E^1 and J_E^2 .

such a phenomenon shown in Fig. 4a should be a vortex line softened by thermal activation. With increasing temperature, the restriction to the vortex lines becomes weaker and weaker, and the transition from a disentangled regime to an entangled regime will occur at last. In terms of this frame, x_0 should be regarded as the effective radius of the vortex line. The increase of x_0 with temperature directly weakens the dependence of U_j on J_c because of $J_c(T) = U_j(T)/x_0(T)$. When x_0 reaches the value of a at T_{tr} , it rises no further, and so the linear relation is gained. This transformation process of the pinning potential well is shown in Fig. 4b, which is in good agreement with the result in Fig. 4a. From the above discussion, we can conclude that T_{tr} is the boundary between the disentangled regime and the entangled regime, i.e. the anticipated GL transition temperature.

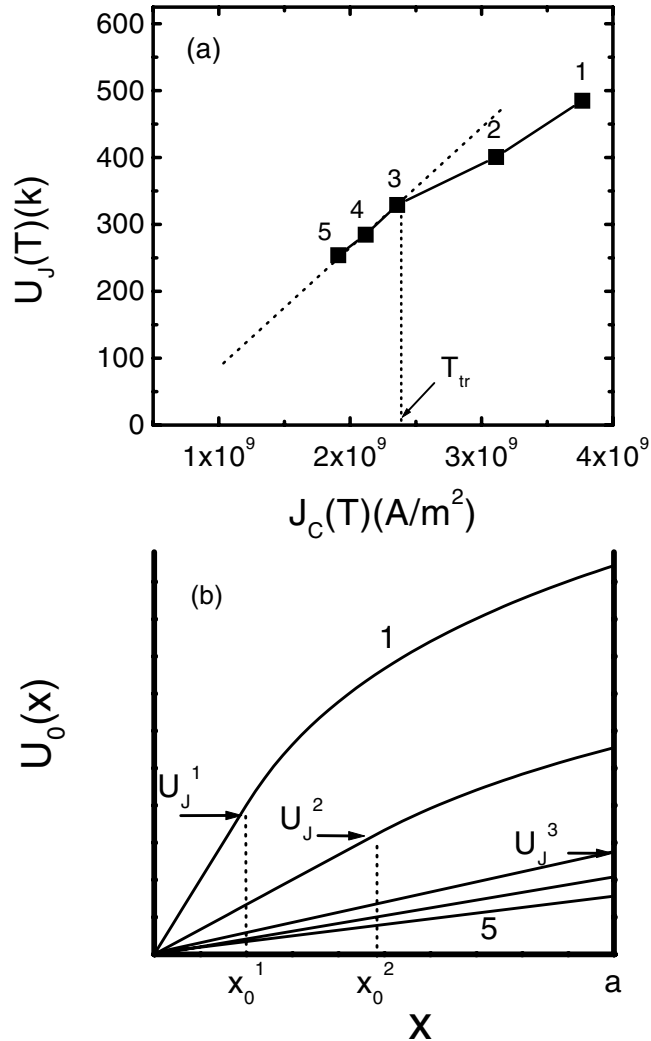


Fig. 4. (a) Relation between $U_J(T)$ and $J_C(T)$ at the fixed magnetic field of 8 T, where T_{tr} is the transition temperature from vortex glass to vortex liquid. Note that the dependence of U_J on J_C is linear when $T > T_{tr}$, but this linearity is destroyed below T_{tr} . (b) Schematic of the changing process for the shape of the pinning potential well. Curves 1 to 5 are for five temperatures increasing by degrees.

Acknowledgments

This work was supported by National Foundation (19974015) and the Ministry of Science and Technology (NKBRFSF-G19990604) of China.

References

- Anderson, P. W. (1966). In 'Quantum Fluids' (Ed. D. F. Brewer), p. 146 (North Holland: Amsterdam).
 Bondarenko, A. V., Shklovskij, V. A., Obolenskii, M. A., Vovk, R. V., and Prodan, A. A. (1998). *Phys. Rev. B* **58**, 2445.

- Brandt, E. H. (1995). *Rep. Prog. Phys.* **58**, 1465.
- Brandt, E. H. (1996). *Phys. Rev. B* **54**, 4246.
- Brandt, E. H. (1997). *Physica C* **282–7**, 343–6.
- Brown, B. (2000). *Phys. Rev. B* **61**, 3267.
- Crabtree, G. W., and Nelson, D. R. (1997). *Phys. Today*, April, p. 38.
- Doyle, R. A., Quinton, W. A. J., Baudenbacher, F., Liang, W. Y. (1998). *Physica C* **308**, 169–74.
- Giamarchi, T., and Le Doussal, P. (1996). *Phys. Rev. Lett.* **76**, 3408.
- Gilchrist, J., and van der Beek, C. J. (1994). *Physica C* **231**, 147.
- Griessen, R., Hoekstra, A. F. Th., Wen, H. H., Doornbos, G., and Schnack, H. G. (1997). *Physica C* **347**, 282–7.
- Gurevich, A., and Brandt, E. H. (1994). *Phys. Rev. Lett.* **73**, 178.
- Higgins, M. J., and Bhattacharya, S. (1996). *Physica C* **257**, 232–54.
- Jakob, G. (1991). *Appl. Phys. Lett.* **59**, 1626.
- Koshelev, A. E., and Vinokur, V. M. (1994). *Phys. Rev. Lett.* **73**, 3580.
- Malozemoff, A. P. (1991). *Physica C* **26**, 185–289.
- Mankiewich, P. M., Howard, R. E., Straughn, B. L., and Burkhardt, E. G. (1989). *Phys. Rev. Lett.* **62**, 2044.
- Mannhart, J., Chaudhari, P., Dimos, D., Tsuei, C. C., and McGuire, T. R. (1988). *Phys. Rev. Lett.* **61**, 2476.
- Rhyner, J. (1993). *Physica C* **212**, 292.
- Schnack, H. G., Griessen, R., Lensink, J. G., and Wen, H. H. (1993). *Phys. Rev. B* **48**, 13178.
- Schuster, Th., Kuhn, H., Brandt, E. H., Indenbom, M., Koblishka, M. V., and Konczykowski, M. (1994a). *Phys. Rev. B* **50**, 16684.
- Schuster, Th., Indenbom, M. V., Kuhn, H., Brandt, E. H., and Konczykowski, M. (1994b). *Phys. Rev. Lett.* **73**, 1424.
- Schuster, Th., Kuhn, H., and Brandt, E. H. (1995a). *Phys. Rev. B* **51**, 697.
- Schuster, Th., Kuhn, H., Brandt, E. H., Indenbom, M. V., Klüser, M., Müller-Vogt, G., Habermeier, H.-U., Kronmüller, H., and Forkl, A. (1995b). *Phys. Rev. B* **52**, 10375.
- Schuster, Th., Kuhn, H., and Brandt, E. H. (1996). *Phys. Rev. B* **54**, 3514.
- Shan, L., Sun, A. M., Xu, X. N., Tang, Y. L., Lu, D. W., Jin, X., Shen, L. J., Lam, C. C., and Chen, Y. S. (1999). *Supercond. Sci. Technol.* **12**, 1138.
- Sueyoshi, T., Ishikawa, N., Iwase, A., Chimi, Y., Kiss, T., Fujiyoshi, T., and Miyahara, K. (1998). *Physica C* **309**, 79–88.
- Vinokur, V. M., Feigel'man, M. V., and Geshkenbien, V. B. (1991). *Phys. Rev. Lett.* **67**, 915.
- Wen, H. H., and Zhao, Z. X. (1995). *Phys. Rev. B* **52**, 4583.
- Yazawa, T., Rabbers, J. J., Ten Haken, B., Ten Kate, H. H. J., Yamada, Y. (1998). *Physica C* **310**, 36–41.
- Zeldov, E., Amer, N. M., Koren, G., Gupta, A., McElfresh, M. W., and Gambino, R. J. (1990). *Appl. Phys. Lett.* **56**, 680.